

Dimensional Analysis of UVGI Air Disinfection Systems

W.J. Kowalski
Member ASHRAE

W.P. Bahnfleth
Member ASHRAE

J.L. Rosenberger

A dimensional analysis of an ultraviolet germicidal irradiation (UVGI) air disinfection system within a diffusely reflective enclosure is performed using the Buckingham pi theorem. The eight dimensionless parameters obtained include the duct aspect ratio, the lamp aspect ratio, the reflectivity, and terms that incorporate the UV dose, airflow, duct dimensions, and lamp location coordinates. Computer simulation of the dose absorbed by an airborne microbe is used to predict system performance for several thousand combinations of the dimensionless parameters. Statistical analysis of these results is performed to determine the significance of each of the dimensionless parameters and their interactions. Conclusions regarding performance are summarized. The most significant parameters that determine performance of diffusely reflective UVGI systems are shown to be the dose, the reflectivity, the duct geometry, the lamp aspect ratio, lamp location, and various combined functions of these parameters. Practical implications of this research may include the improvement or optimization of UVGI air disinfection systems for in-duct and recirculation unit applications, with a consequent improvement in energy efficiency.

INTRODUCTION

UVGI systems are in common use for disinfecting air, surfaces, and water and are a major weapon in the fight against disease transmission. Water-based UVGI systems have a history of reliability and predictability, but the same is not true for air disinfection systems, the design of which has primarily been guided by experimental results and a limited number of studies. The limited understanding of the design principles has resulted in many UVGI installations that are either overdesigned and inefficient or underdesigned and ineffective. Analytical methods for predicting UVGI system performance have recently been developed (Kowalski and Bahnfleth 2000), but a complete evaluation of the factors that contribute to effective design of such systems has not previously been performed. A closed-form solution of the UVGI disinfection process does not exist and is probably not feasible, so the influence of system parameters must be deduced from the results of parametric studies. Dimensional analysis, widely applied in fields such as fluid mechanics and convective heat transfer, provides a convenient and powerful method for analyzing the voluminous results of such studies.

Dimensional analysis involves the definition of all relevant dimensional variables for any system and identification of the minimum number of independent dimensionless parameters that can be produced from these variables. The Buckingham pi theorem is a formal method for identifying the dimensionless parameters and is the approach used here.

Figure 1 illustrates the geometry and dimensions of the representative UVGI system. Only single lamps are considered in this study. A UV lamp is installed in the duct in a cross-flow arrangement with the contaminated air passing through it. The coordinate system used throughout is $z = 0$ at the front face of the duct, $x = 0$ at the left side of the duct, and $y = 0$ at the bottom

W.J. Kowalski is a research associate and **W.P. Bahnfleth** is associate professor and the director of the Indoor Environment Center, Architectural Engineering Department, The Pennsylvania State University, University Park, Penn. **J.L. Rosenberger** is a professor and head of the Department of Statistics, Pennsylvania State University, University Park, Penn.

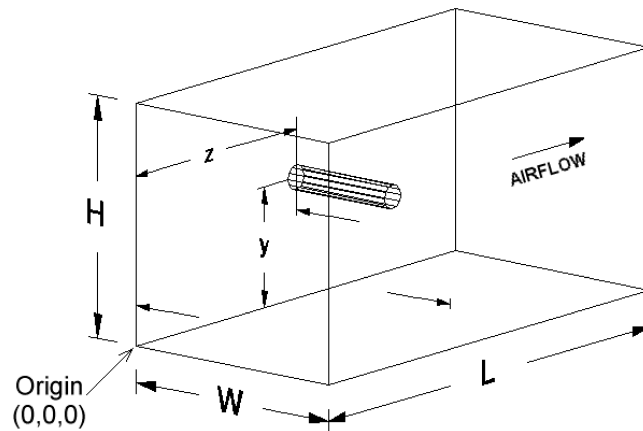


Figure 1. Geometry and Dimensions of a Rectangular UVGI System; the Lamp Length = x and Airflow Is Along the Length L

side of the duct. The left end of the lamp is considered to be at $x = 0$; therefore, x is equivalent to the lamp arclength.

The physical parameters that define performance and operation of UVGI systems are listed in Table 1. The generic units shown in the table include T = time, L = length, M = mass, and D = degrees (temperature). The x , y , and z coordinates represent the location of the lamp within the rectangular duct. The x coordinate of the lamp end is identical to the lamp arc length when the base of the lamp is at $x = 0$. The rate constant k defines the response of any microbial population under UV irradiation in accordance with the exponential decay equation:

$$\ln S = -kI_{avg}t \quad (1)$$

where

- S = survival, fractional;
- k = rate constant, $\text{cm}^2/\mu\text{W}\cdot\text{s}$;
- I_{avg} = average UVGI irradiance, $\mu\text{W}/\text{cm}^2$;
- t = exposure time, s.

Some parameters in this model can or must be neglected due to limited quantitative information on their effects. These include air temperature, relative humidity, photoreactivation effects, and specular reflectivity. The air temperature has a negligible impact on microbial survival during UVGI irradiation provided that neither freezing nor heat damage occurs (Rentschler et al 1941). This would be true for most constant volume ventilation systems since the air temperature tends to remain in a narrow range between approximately 13°C and 27°C (55°F - 80°F), depending on location and other factors.

Air temperature can also impact UV lamp output by overcooling the lamp, especially when air velocity is beyond design limits. Most UV lamps are designed to operate, and are rated, at an air temperature of approximately 21.5°C (70°F) and an air velocity of 2-2.54 m/s (400-500 fpm). Lamp UV output may decrease or increase outside this range. Some lamps can lose 25% or more of their UV output when the air temperature drops from 27°C (80°F) to 16°C (60°F) (Westinghouse 1982). Certain UV lamps have controls that will boost UV output in response to the cooling effects of airflow (Kowalski and Bahnfleth 2000). Still other lamps may include a UV-transparent shield to reduce cooling effects. There are well over one hundred different types of UV lamps, and their individual performances cannot be generalized. The present analysis is

Table 1. Defining Parameters of UVGI Air Disinfection Systems

Parameter	Description	Units
W	Duct width	L
H	Duct height	L
L	Duct length	L
r	Lamp radius	L
<i>l</i>	Lamp arc length (= x, the lamp end coordinate)	L
P	Lamp UV power	ML ² /T ³
t	Exposure time	T
x	Lamp end coordinate (= lamp arc length w/ base at x = 0)	L
y	Lamp Y position or distance above bottom surface	L
z	Lamp Z position or distance from duct entrance	L
Re	Degree of air missing or turbulence, Reynolds number	
k	UVGI rate constant	T ² /M
T	Air temperature	D
RH	Relative humidity	
PR	Photoreactivation rate (in open air and visible light)	1/T
ρ	Surface reflectivity	
Q	Airflow rate	M ³ /T
S	Survival fraction	

based on UV output, not the performance of particular lamps, under varying conditions, and, therefore, lamp cooling effects are not addressed here. The air velocity in this analysis is kept at the typical design limit of 2.54 m/s (500 fpm).

The effect of relative humidity (RH) on the rate constant has long been a matter of debate. Some studies have shown that for some species the UV decay rate decreases with increased RH (Riley and Kaufman 1972; Lidwell and Lowbury 1950) while other studies show that the decay rate under UV exposure increases with increased RH (Rentschler and Nagy 1942). A recent study indicates that the decay rate decreases with increasing RH for three bacterial species under UV exposure (Peccia et al. 2001). At present there are insufficient data available to quantify the effects in any general way, and so the effects of RH are not included in this study. In indoor environments, ASHRAE (1993) defines comfort zones as having an RH below 60%, and this would be the operating RH range of any UVGI system that recirculated room air or disinfected return air. In an air-handling unit, however, the RH could vary greatly depending on where the UVGI system was located. Obviously, RH effects may dictate the preferred location of any installed UVGI system and may even allow a means of boosting UVGI efficiency through RH control, but without further quantitative results on RH effects, no detailed modeling of RH effects is possible in this study.

Another factor that cannot be adequately addressed at present is the phenomenon of photoreactivation. Photoreactivation occurs when microorganisms are exposed to visible light during or after UV irradiation (Setlow 1966). This process can result in self-repair of damaged microbes and can cause a significant percentage of the population to recover from UV inactivation. Photoreactivation has been studied at length in water-based UV experiments, but the data for photoreactivation of airborne microbes are limited at present (Linden and Darby 1994). One study indicates the decay rate of *Mycobacterium parafortuitum* under UV exposure in liquid suspension is effectively decreased by simultaneous exposure to visible light (Peccia and Hernandez 2001). The same study suggests that airborne microbial populations can recover significantly if

allowed sufficient time. The photoreactivation effect may be dependent on RH, with the effect absent when RH is less than approximately 65% (Peccia and Hernandez 2001). Evidence suggests that a conformational DNA change occurs above some discrete range of RH that may allow microbes to experience photoreactivation (Rahn and Hosszu 1969; Munakata and Rupert 1974).

Although no general quantitative model for photoreactivation of airborne microbes exists at present, some considerations for the design of UVGI systems can be given based on what is known about the photoreactivation effect. Ideally, the RH would be kept below approximately 65% in any UVGI system, and the UVGI enclosure should admit little or no internal visible light. Also, the recovery time during which photoreactivation may occur is a function of the mean residence time of building air (for systems that recirculate air). Although the mean residence time cannot easily be manipulated, it can be accounted for by use of the air change rate and the photoreactivation rate at such time that data become available. In Table 1, the photoreactivation rate, PR, has the units of inverse time (1/T), since it would be defined by the percentage (or fraction) of the population that was reactivated over time during exposure to visible light in open air. The impact of photoreactivation on the UVGI rate constant must be defined separately and would be dimensionless.

Reflectivity may have two components, diffuse and specular,

$$\rho = \rho_d + \rho_s \quad (2)$$

where

ρ_d = diffusive reflectivity, fractional, and

ρ_s = specular reflectivity, fractional.

In the computer model on which this analysis is based, reflectivity is assumed to be diffusive and to have no specular component. Most real-world materials, such as galvanized duct, include both diffusive and specular components. Polished aluminum is almost entirely specular, while reflective materials, such as magnesium oxide or ePTFE, are almost perfectly diffusive. Results of this analysis must be considered to apply to diffuse reflectivity only.

The effects of air mixing are bounded by conditions of completely mixed and completely unmixed flow, and, therefore, flow parameters such as the Reynolds number are omitted from the model (Kowalski and Bahnfleth 2000). The exposure time is an implicit result of the airflow and duct dimensions and is not needed as a separate independent variable.

The analysis of system performance depends on the use of a program developed by at Penn State that simulates the three-dimensional (3D) intensity field inside a reflective enclosure and its effects on airborne microbes in an airstream passing through it (Kowalski 2001). This software, called the UVX program, predicts the performance of a rectangular UVGI system with internal diffuse reflective surfaces and any number or type of UV lamps. The program employs thermal radiation view factors to evaluate the lamp intensity field and the intensity field due to diffuse reflections. The computer models of the lamp and the reflective surfaces approximate the UV flux, or spherical irradiance, that would be experienced by an airborne spherical microbe.

Program predictions have been verified independently by three different laboratories in 25 bioassays on *Serratia marcescens*, 6 bioassays of *Bacillus subtilis*, 2 bioassays on *Streptococcus pneumoniae*, and 2 bioassays on *Mycobacterium parafortuitum* to within an accuracy of approximately $\pm 30\%$ (Kowalski 2001; UVDI 2002). The accuracy in these tests was better than $\pm 12\%$ in 85% of the cases, with only a single test out of 35 being rejected from the complete set as anomalous. A wide variety of operating conditions, duct sizes, and lamp configurations have been tested and the ability of the model to predict the survival of airborne microbes under UV exposure in rectangular reflective ducts remains within the stated accuracy limits under varia-

tions of all of the defined parameters. Attempts to calibrate the reflectivity model using spherical actinometry (Rahn et al. 1999) have been inconclusive so far.

In this study a modified version of the UVX program is used to predict the performance of UVGI system configurations based on most of the variables in Table 1. In effect, the program is used in lieu of laboratory tests without the associated time and expense. This approach may lack absolute empirical veracity, but it can rapidly and exhaustively analyze more system configurations than could ever be feasibly tested in a laboratory.

Table 2 gives examples of data input and output for the program. All the other variables shown are as defined in Table 1 except the kill rate, K , which is computed as follows

$$K = 1 - S \tag{3}$$

DIMENSIONAL ANALYSIS

The minimum set of defining system variables for this model is summarized in Equation 2 in terms of the natural logarithm of the survival.

$$\ln S = \phi(W, H, L, r, P, t, x, y, z, k, \rho) \tag{4}$$

The flow rate Q is not included in Equation 4 since the exposure time t and the duct dimensions also define the airflow. The flow rate Q is reintroduced later as a useful simplification of one of the dimensionless parameters. The lamp arc length is not included in Equation 4 since it is equivalent to the x coordinate of the lamp, as stated previously (Figure 1). These terms, l and x , will be used interchangeably in this study.

The formal analysis proceeds with application of the Buckingham pi theorem (Kundu 1990). The first step is to establish the number of dimensional parameters and the number of repeating units. There is a total of 12 parameters in Equation 4, but only 10 of these parameters have dimensions, so the total number n is 10. Table 3 summarizes the dimensions of each parameter in the generic M, L, and T unit system (i.e., mass, length, and time), excluding S and r since these are already dimensionless. Since there are only three repeating units (M , L , and T), the number of repeating parameters is $m = 3$.

The parameters rate constant (k), power (P), and length (L) are selected as the three repeating parameters. These parameters embody the three dimensions M , L , and T . Combinations of the repeating parameters with other parameters form groups with dimensions $M^a L^b T^c$ in which the exponents of the parameters are determined algebraically to make the exponents a , b , and c identically zero.

According to the Buckingham pi theorem, the minimum number of unique dimensionless pi groups is $n - m$, or 7 in the present case. For the first pi group, kPLW:

$$\left(\frac{T^2}{M}\right)^a \left(\frac{ML^2}{T^3}\right)^b (L)^c (L) = M^0 L^0 T^0 \tag{5}$$

Equating the exponents yields $a = 0$, $b = 0$, and $c = -1$. The first pi group is, therefore,

$$\Pi_1 = \frac{W}{L} \tag{6}$$

In similar fashion, the remaining pi groups can be determined. The natural logarithm of the survival is summarized as a function of the seven pi groups and the eight dimensionless parameters r as follows:

Table 2. UVX Program Sample Input and Output Data

Program Input Data											Output	
W cm	H cm	r cm	I cm	k cm ² /mW·s	P W	t s	x cm	y cm	z cm	L cm	ρ %	Kill Rate %
241	240	0.59	128	0.0028	4	5.59	128	61	60	120	0.65	65
295	204	0.72	156	0.0028	4	5.79	156	52	60	120	0.65	64
349	184	0.85	185	0.0028	4	6.18	185	47	60	120	0.65	63
349	184	7.56	185	0.0028	4	6.18	185	47	60	120	0.65	63
402	172	0.98	213	0.0028	4	6.66	213	44	60	120	0.65	63
456	164	1.11	241	0.0028	4	7.19	241	42	60	120	0.65	62
509	158	1.24	270	0.0028	4	7.74	270	40	60	120	0.65	62
563	153	1.37	298	0.0028	4	8.31	298	39	60	120	0.65	62

Table 3. Array of Units for UVGI System Minimum Parameters

Unit	W	H	L	r	P	t	x	y	z	k
M	0	0	0	0	1	0	0	0	0	-1
L	1	1	1	1	2	0	1	1	1	0
T	0	0	0	0	-3	1	0	0	0	2

$$\ln S = f\left(\frac{W}{L}, \frac{r}{L}, \frac{kPt}{L^2}, \frac{x}{L}, \frac{y}{L}, \frac{z}{L}, \frac{H}{L}, \rho\right) \quad (7)$$

More useful combinations can be created from the parameters shown in Equation 7 that will be more practical to use and more intuitive, such as the duct aspect ratio and the lamp aspect ratio. The duct aspect ratio can be formed from pi groups 1 and 2:

$$\Pi_a = \frac{\Pi_1}{\Pi_2} = \frac{WL}{LH} = \frac{W}{H} \quad (8)$$

The lamp aspect ratio, Y ratio (y/H), and H ratio (H/L) can be formed with similarly trivial algebra. The fifth pi group, which includes the lamp power, can be modified by multiplying pi groups 1 and 2 and making an appropriate conversion:

$$\Pi_5 = \frac{kPt}{L^2} \Pi_1 \Pi_2 = \frac{kPt}{L^2} \left(\frac{L}{W}\right) \left(\frac{L}{H}\right) = \frac{kPt}{WH} \quad (9)$$

This pi group can be made into an even more useful form, one that incorporates both the airflow Q and the length L , by defining the exposure time in terms of the volume and flow rate and multiplying by pi groups 1 and 2. Because of its general form, which includes UV power per unit of airflow, the resulting term is called the specific dose.

$$\Pi_5 = \frac{kPt}{L^2} \Pi_1 \Pi_2 = \frac{kP}{L^2} \left(\frac{WHL}{Q}\right) \left(\frac{L}{W}\right) \left(\frac{L}{H}\right) = \frac{kPL}{Q} \quad (10)$$

Analysis and interpretation can be further simplified by substituting the kill rate K for the survival S . The relationship between the natural log of the kill rate and the eight dimensionless parameters is

$$\ln K = f\left(\frac{W}{H}, \frac{r}{l}, \frac{kPL}{Q}, \frac{x}{W}, \frac{y}{H}, \frac{z}{L}, \frac{H}{L}, \rho\right) \quad (11)$$

In Equation 11, the lamp arc length has been substituted for the x coordinate in the second pi group since these are equivalent. The range of values for the dimensionless parameters in Equation 11 is shown in Table 4, along with the maximums and minimums used in this study. These limits were selected as being representative of some of the most extreme values that might be encountered in actual installations, but they are by no means absolute limits. The duct aspect ratio, for example, can go from $W/H = 1$ (square duct) to a practical maximum of about 5. The range for the lamp aspect ratio was established by reviewing actual lamp dimensions. These are available from various sources including catalogs and handbooks (IES 1981).

The range for the specific dose was selected to produce kill rates in the range of 1% to 99%. As kill rate approaches 100%, its sensitivity to increasing UV power vanishes, so kill rate must be held below approximately 99% to have any significance. The X ratio minimum is based on the shortest available lamp and the maximum represents a full span of the duct. The Y ratio is limited by assuming the lamp will be no closer than approximately one lamp diameter and that the maximum Y ratio is limited to 0.5 because of symmetry. The Z ratio limits are arbitrarily selected to span 90% of the duct length. The reflectivity ranges between zero (no reflective surface or open air) and an upper limit of approximately 99.9% (Lash 2000).

FACTORIAL ANALYSIS

In any air disinfection application, the objective is to maximize $\ln K$ in Equation 11. The relative importance of the parameters in determining overall kill rate can be determined by performing a 2^k factorial analysis (Montgomery 2001). The 2^k factorial analysis involves establishing a high and a low value for each of the k parameters and analyzing all of the resulting 2^k permutations. For the present analysis with eight parameters, the number of permutations is therefore 256.

The ten dimensional variables were assigned values that span a range of minimums and maximums as shown in Table 5. The lamp coordinate x_2 represents the end of the lamp (the lamp length) since the other lamp coordinate is at $x = 0$. The values for exposure time and air velocity are shown for information only.

Table 4. Dimensionless Parameters and Limits

Parameter	Description	Practical Range	
		Min	Max
W/H	Aspect ratio	1	5
r/l	Lamp aspect ratio	0.005	0.041
kPL/Q	Specific dose	0.014	2.1
x/W	X ratio	0.063	1.0
y/H	Y ratio	0.008	0.5
z/L	Z ratio	0.10	0.90
H/L	H ratio	0.100	2.0
ρ	Reflectivity	0.00	0.999

Table 5. Variable Minimum and Maximum Values

Variable	Minimum	Maximum	Units	Description
W	1	3448	cm	Width
H	5	1148	cm	Height
L	1	2584	cm	Length
l	0.15	396.45	cm	Lamp arc length
x	0.15	396.45	cm	Lamp x2 coordinate
r	1.00	1.00	cm	Lamp radius
P	0.1464	396.45	W	UV power
y	0.12	292	cm	Lamp y coordinate
z	1.60	574	cm	Lamp z coordinate
k	0.00275	0.00275	cm ² /μW·s	Rate constant
ρ	0.0	0.990		Reflectivity
Q	3.05	292	m ³ /min	Airflow
t	0.0321	4.52	s	Exposure time
V	2.54	2.54	m/s	Velocity

Table 6. Star Points and Center Points for Input Parameters

Case	W/H	r/l	kPL/Q	x/W	y/H	z/L	H/L	ρ
Lo Star	1.00163	0.005	0.036	0.06	0.008	0.10	0.024	0.005
Min	1.588	0.010	0.390	0.200	0.080	0.220	0.310	0.15
Center	3.004	0.023	1.245	0.530	0.254	0.500	1.000	0.50
Max	4.420	0.036	2.100	0.860	0.428	0.780	1.690	0.85
Hi Star	5.0	0.041	2.5	1.0	0.500	0.90	2.0	0.9949

Some variables were held constant to provide for practical interpretation and comparison. The rate constant shown in Table 5, 0.00275 cm²/μW·s, represents *Serratia marcescens*, which was used as a design basis airborne pathogen in previous studies (Kowalski 2001; Kowalski et al. 2000). The air velocity was held constant at a value of 2.54 m/s (500 fpm). The lamp radius was held constant at 1 cm. Although the lamp radius could vary from 0.79 cm to about 2 cm, it was necessary to hold one value constant as a means of computing all other parameters, and the radius was deemed the most practical parameter since it is the smallest and had the narrowest range.

The 2^k factorial data set, which was output by the UVX program, is complete and in standard order, and it was analyzed as a general linear model (Montgomery 2001). This analysis considered all two-way, three-way, four-way, and five-way interactions between the dimensionless parameters. The analysis of variance (AOV) of lnK indicates that the specific dose is the most influential factor and that most of the interactions are of negligible importance.

The AOV indicated that higher-order functions were involved, and a final statistical analysis was performed using response surface methodology (RSM) on a central composite design (CCD) using a second-order model (Montgomery 2001). In addition to the 256 data sets from the 2^k factorial screening analysis, additional points known as center points and star points are included as shown in Table 6.

The center point for this model is the set of all medians of the dimensionless parameters. Normally, multiple center points would be added in laboratory tests so as to provide an accurate estimate of the random error. However, in this case there is no random error since the computer

program will always produce identical results for a given set of inputs, and, therefore, only one center point is needed.

The star points are determined by taking the distance of the minimum (low) or maximum (high) value of each dimensionless parameter and multiplying by a constant called alpha, typically with a value of $\sqrt{2}$ as in this case. This value is commonly used to represent a balanced set of data points encircling a square (in two dimensions) that defines the high and low points.

The 256 data sets from the 2^k factorial analysis were augmented with the star points and center points from Table 6, and these were analyzed using commercial statistical analysis software (Minitab 2000). Table 7 summarizes the results for the eight primary parameters, all interaction parameters, and all higher-order terms that explained 0.1% or more to the total sum of squares error (SSE), along with the analysis of variance (AOV) results. The function coefficients, the second column of Table 7, are the multipliers of the functions in the first column. The sequential sum of squares (SS) is shown in the third column, the percent (%) of the total SSE in the fourth column, and the statistical P-values are shown in the final columns. The summary at the bottom

Table 7. Analysis of Variance and Coefficients

Parameter Function	Function Coeff.	Sequential SS	% SSE	P Value
Constant	-5.5958	-		0
W/H	0.0277	0.0206	0.01	0.629
r/l	-0.8097	0.028	0.02	0
kPL/Q	-20.722	85.0091	56.45	0
x/W	-0.2462	0.4656	0.31	0.19
y/H	0.0222	0.0369	0.02	0.945
z/L	2.6413	33.3581	22.15	0
p	0.6976	0.0049	0.00	0.005
H/L	-11.1739	15.1256	10.04	0
(kPL/Q) ²	7.859	3.1206	2.07	0
(x/W) ²	0.2761	0.2861	0.19	0.116
kPz/Q	-0.58384	3.275	2.17	0
kPH/Q	-0.114101	1.16	0.77	0
xz/WL	-0.54691	0.2935	0.19	0
yz/HL	-1.23362	0.5398	0.36	0
zH/L ²	-0.42965	2.7562	1.83	0
(kPL/Q) ³	-1.4573	1.5834	1.05	0
sqrt(kPL/Q)	20.715	0.1952	0.13	0
atan(H/L)	16.2651	1.4054	0.93	0
(H/L) ³	0.91925	0.8165	0.54	0
S = 0.04987 R - Sq = 99.50% R - Sq (adj) = 99.40%				
Source	DF	SS	MS	P
Regression	28	150.2	5.36	0
Residual	44	0.246	0.0017	
Total	272	150.6		

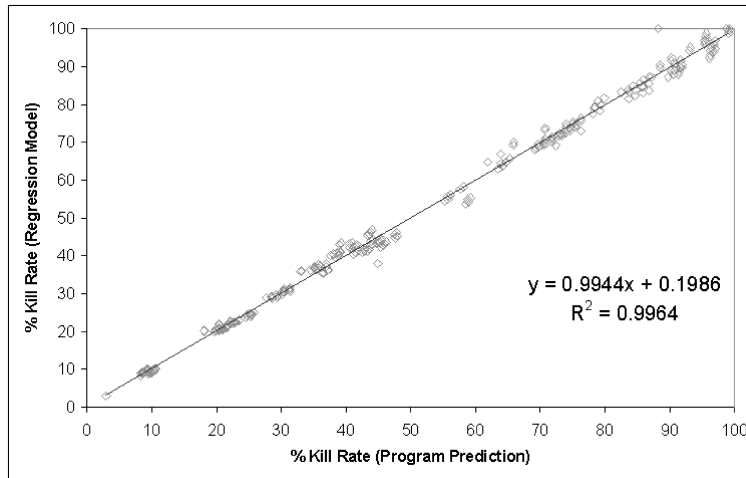


Figure 2. Predicted Kill Rate for Regression Model

of Table 7 shows the degrees of freedom (DF), the sum of squares, mean square (MS), the fit test (F) statistic, and the probability P value. P values of less than 0.0005 are shown as zeros in Table 7.

The normal probability plot of the data indicated reasonably good fit to the data with only small deviations in the extremes. Figure 2 shows the results for the 273 data sets from the statistical evaluation and illustrates the predictive ability of the regression model. This regression model uses the coefficients and parameter functions from Table 7. The data sets were used as input and the kill rates predicted by the program were compared against the kill rates predicted by the linear regression model.

Although the regression model adequately predicts kill rates within the factorial analysis data set, it was found to be less successful at predicting random data sets and is not by itself a good substitute for the program. The real value of this regression model lies in what it reveals about the importance of the various system parameters.

The most significant first-order parameters, based on P values less than 0.005, are the specific dose, the lamp aspect ratio, the Z ratio, the reflectivity, and the height ratio. The main conclusion of this regression model analysis is that there is little significant interaction between any of the dimensionless parameters. Taken together, the parameters and functions in Table 7 account for more than 97% of the predictive ability of the regression model.

RESULTS OF ANALYSIS

In this section the various dimensionless parameters are studied to determine how they affect performance individually and how they might be manipulated. Because the interactions between the eight dimensionless parameters have little significant impact, these parameters can be optimized independently of each other to maximize kill rate for a given UV power and airflow. Therefore, a comparison of the parameters on a one-to-one basis (e.g., with each parameter compared against each other parameter with all others held constant) provides insight into the relative significance and behavior of each parameter. For each pair of parameters, 100 analyses were run and plotted to create response surfaces (contour plots) for kill rate. The most important contours are summarized here.

Figure 3 shows the response surface for kPL/Q , the specific dose, vs. W/H , the duct aspect ratio. This figure suggests the duct aspect ratio has a negligible effect on kill rates, although there is a slight peak at approximately $W/H = 2.0$. Figure 3 also shows that the kill rate responds nonlinearly to an increase in the specific dose, and the rate of increase levels off as the specific dose is increased. In fact, this rate of decrease is exponential and is a direct result of the characteristic exponential decay curve of Equation 1.

Figure 4 shows that the kill rate responds in an approximately linear fashion to an increase in reflectivity for all values of the duct aspect ratio. Comparing this to Figure 3, where the kill rate levels off above some point, it can be concluded that beyond some power level there is more to be gained from increasing reflectivity than from increasing power. Again, there is a very slight

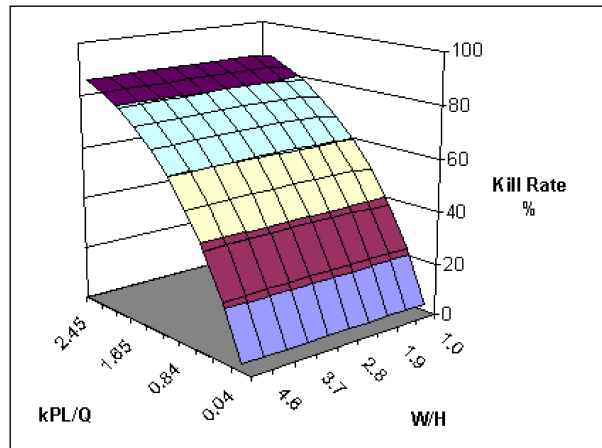


Figure 3. Kill Rate for Specific Dose vs. Duct Aspect Ratio

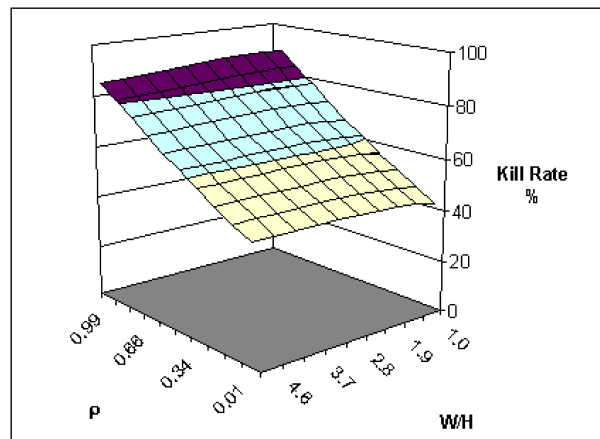


Figure 4. Kill Rate for Reflectivity vs. Duct Aspect Ratio

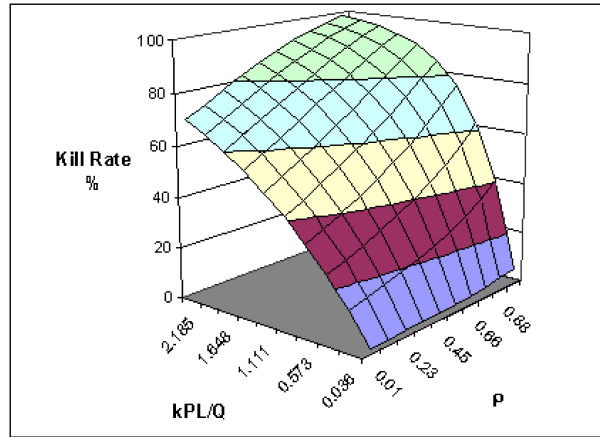


Figure 5. Kill Rate for Specific Dose vs. Reflectivity

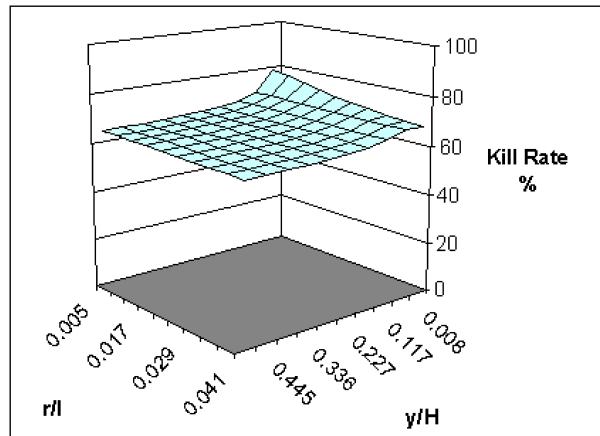


Figure 6. Kill Rate for Lamp Aspect Ratio vs. Y Ratio

increase in kill rate at a duct aspect ratio of greater than approximately 2.0, but the increase is hardly significant, especially in light of the program accuracy limitations.

Figure 5 compares the effects of reflectivity and specific dose. Increasing reflectivity produces an approximately linear increase in kill rates at the lowest values of specific dose, but the gains level off at higher specific doses. This response is due to the fact that kill rates level off near 100%. It is not too difficult to see from this chart that if the same kill rates can be achieved by increasing reflectivity, then the expense of increasing lamp power may be unnecessary. However, this is a matter that must be left for a detailed economic evaluation.

Figure 6 plots the Y ratio vs. the lamp aspect ratio. This figure shows an interesting effect – the kill rate increases by almost 15% as the lamp is moved toward the diffusive reflective surface. This counterintuitive phenomena is termed the *proximity effect*. It is an interesting result

because common industry practice is to place UV lamps in the central location in a duct. This boost in system efficiency also comes for no additional cost, since it merely involves placement of the lamp. It is not known exactly how close a lamp can actually be placed near the surface since airflow between the lamp and the duct will experience interference at some point. This matter remains to be studied further, but it is assumed that, for practical purposes, the limit is approximately one lamp diameter at design air velocity. Because there must be a limit to how close a lamp can be placed to a reflective surface before interference with the airflow occurs, it can be hypothesized that an optimum Y ratio must exist for any given UVGI diffusely reflective system configuration. Figure 6 also indicates that the lamp aspect ratio influences the proximity effect and has an optimum at low values in this regard.

Preliminary studies on specular reflective surfaces show an opposite proximity effect – optimum placement of lamps is away from the specular reflective surfaces. This can be explained by the fact that the more concentrated intensity fields produced by specular reflections, as opposed to diffuse reflections, represent an inefficient distribution of the local intensity field for the purpose of inactivating microorganisms. More study needs to be done on specular surfaces, however, and the model evaluated here is strictly for diffusive surfaces.

Figure 7 shows the response surface for the X ratio vs. the Y ratio. The X ratio is the arc length of the lamp divided by the duct width (Figure 1). The kill rate is boosted by about 15% as the lamp length is shortened relative to the duct width. Although this effect is similar to the proximity effect of the Y ratio, it is not produced by a local increase in average intensity but from an improvement in system efficiency resulting from geometry. The combined minimization of both the Y ratio and the X ratio results in a maximum 25% boost in the kill rate. Of course, if the diffuse reflectivity were low, there may be little to be gained from the proximity effect. However, it is entirely likely that a UVGI system can be engineered to benefit from the proximity effect in many cases. Clearly, the manipulation of the proximity effect in diffusely reflective enclosures can result in considerable energy savings since it would permit reducing lamp power in a nonlinear proportion to the gains from increasing the kill rate (Figure 3).

Figure 8 shows the response surface of the Z ratio vs. the specific dose. The Z ratio represents the depth within the duct at which the lamp is placed (Figure 1). The Z ratio varies from a minimum of 0.1 at approximately the face of the duct inlet, to a maximum of 0.9 at approximately

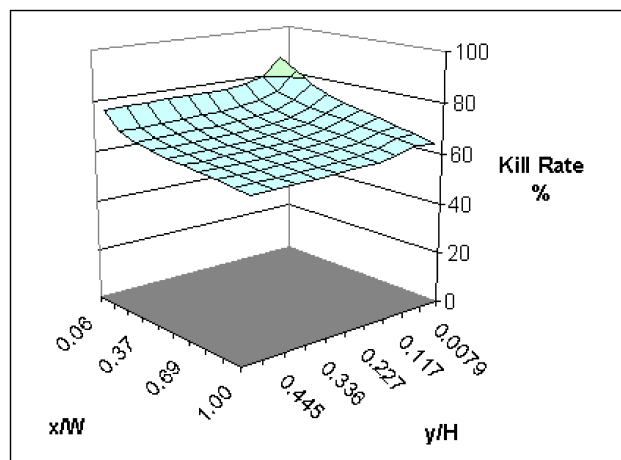


Figure 7. Kill Rate for X Ratio vs. Y Ratio

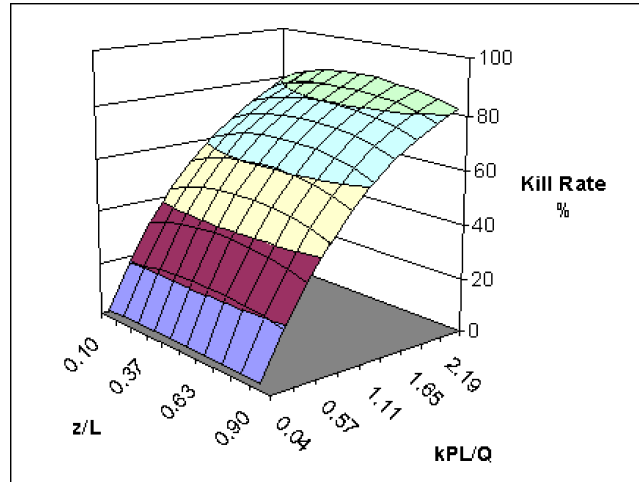


Figure 8. Percent Kill Rate for Z Ratio vs. Specific Dose

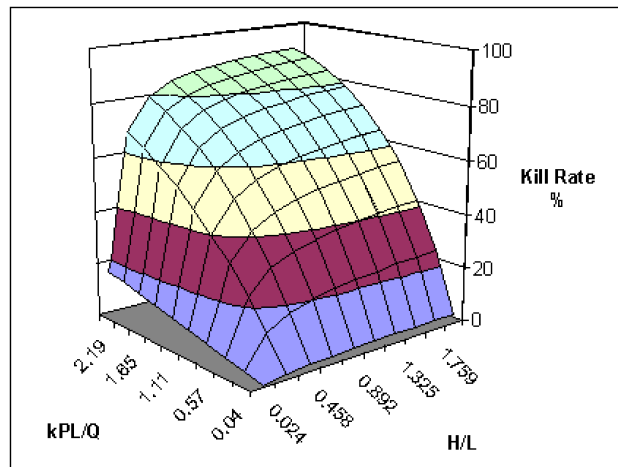


Figure 9. Percent Kill Rate for H Ratio vs. Specific Dose

the duct outlet. The maximum kill rate clearly occurs at a Z ratio of 0.5, or exactly centered along the length of the duct. Since it is common industry practice to locate lamps at the middle portion of any duct, intuition proves to be correct in this case.

Figure 9 shows an example of the eighth parameter, the height ratio, vs. the specific dose. The H ratio is the ratio of the height of the duct face to the duct length. Like most of the parameters, the height ratio contour shows the same result regardless of which parameter it is graphed against. Figure 9 would seem to suggest that a duct that is shorter than the height provides higher kill rates, but the optimum length is more correctly determined by economics. That is, the true optimum value of H/L cannot be ascertained on the basis of the kill rate alone, since it depends heavily on the economics. Prior economic analysis has indicated that an optimum length exists

for any given set of UVGI system parameters (Kowalski 2001). Therefore, no definitive conclusions can be drawn from the dimensionless analysis results for the H ratio.

No further examples need be presented here because the remaining response surface comparisons merely recombine the effects already described, and the critical relationships have been adequately summarized by the previous examples.

PERFORMANCE OPTIMIZATION

The previous results allow for some generalization of the conditions under which performance of rectangular, ducted UVGI systems can be optimized. The aspect ratio produces small increases in the kill rates when it is above some value in the range of 2-4, but the increase in kill rates is on the order of a fraction of a percent and is not significant. The Z ratio will produce optimum kill rates when it has the median of 0.5. The lamp aspect ratio produces optimum kill rates in conjunction with the proximity effect when minimized.

The X ratio will produce optimum kill rates if it is minimized. However, if it cannot be made less than 0.5 then it should be maximized. This is due to the fact that, when a lamp spans the entire width, the proximity effect operates at both ends. Real-world conditions may limit the situations in which the X ratio can be minimized because lamps come only in discrete lengths, and shorter lamps have disproportionately lower power output.

The Y ratio produces optimum kill rates when minimized, although it is difficult to define the optimal value since placing a lamp too close to a surface would reduce local airflow between the lamp and the surface. It is assumed in this study that a lamp can be no closer than one diameter from a surface under design air velocity 2-2.5 m/s (400-500 fpm) without causing a major restriction of the airflow between the lamp and the surface, based on a review of the flow fields around cylinders (Kundu 1977; Gordon 1978). The optimum Y ratio is a matter for future research.

In Figures 3 through 9, all eight parameters have been exhibited. In most of the comparisons, the optimum is obvious and unique at the point of highest kill rate. In addition to the eight parameters evaluated here, the remaining parameter not included in this model, relative humidity, can be surmised to have some optimum value or range based on the previously mentioned studies, including the photoreactivation studies. The optimum relative humidity may be below 65% RH, although it is not yet clear that this applies to all species or airborne microbes. In addition, air temperature and air velocity are factors that affect lamp UV output, and, although the effects cannot be generalized for all lamps, most lamp operating conditions require air temperature and air velocity to remain within some range or below some value to maintain lamp UV output.

Although this theoretical analysis of the dimensionless parameters of diffusely reflective UVGI systems provides considerable insight, practical applications may be limited for the reasons that most UVGI installations have little room for manipulation of design parameters. In one recent installation reviewed by the authors, it was deemed necessary to boost the kill rate for a margin of safety. The kPL/Q value was approximately 1.35 and the reflectivity was 0.54 (or 54%), giving a kill rate of about 70% (Figure 5). Instead of the costly approach of adding lamps or increasing lamp power, it was recommended to add aluminum sheeting and boost the reflectivity to 75%, which increased the kill rate to about 80% without significant additional cost. To obtain a corresponding increase in the kill rate, a kPL/Q of about 1.78 would have required an increase in UV watts of approximately 32%. The latter option would have been considerably more expensive, representing about 50 additional UV watts.

CONCLUSIONS

The dimensional analysis described here has identified eight parameters that are critical for optimizing the performance of rectangular UVGI air disinfection systems with diffuse reflective surfaces. Statistical analysis has determined that interactions are not significant in most cases. Without significant interaction, most of these parameters can be independently manipulated and optimized to improve system performance.

Analysis of these dimensionless parameters has led to some interesting conclusions. Principal among these is the identification of the proximity effect – the phenomenon that locating lamps close to diffusive reflective surfaces can increase the average intensity of the enclosed UV field. The proximity effect can be manipulated in diffusive reflective systems at no cost and can result in a 25% or greater increase in system efficiency and a proportional savings in energy due to reduction in lamp power. Although this may not apply to the more common specularly reflective systems, it could be used to advantage in an in-duct or recirculation UVGI system by locating the UV lamps nearer the sides than in the center as they are most often placed.

An additional observation is that above some level of performance (i.e., 50% kill rate), the gains in kill rate due to increasing power diminish in comparison to the gains to be had from increasing reflectivity. In other words, once some minimum level of power input has been defined for any given system, it is more beneficial to increase reflectivity than to increase UV lamp power. This can also result in energy savings in an optimized system. A practical application of this principle would be the specification of highly reflective panels, either diffuse or specular, in any UVGI system to enhance effectiveness or to decrease lamp and operating costs.

Additional research remains to be done in several areas. The reflectivity model is based on diffuse reflective surfaces, and no quantitative conclusions can be made regarding specular surfaces until specular models are further developed and explored. The manipulation of RH to obtain high decay rates and minimize photoreactivation effects is another area that demands further research. The exact distance that a lamp may be placed close to a reflective surface is limited by fluid mechanics considerations, and this is also left for future research.

The theoretical results and conclusions presented here remain to be corroborated through microbiological testing. Ongoing research by the authors will further develop and implement the conclusions of this study, with the ultimate goal being the development of a fully optimized UVGI system that minimizes energy consumption and maximizes system performance. Such research will lead to more cost-effective air disinfection systems that may provide for reduced incidence of airborne disease in indoor environments and improved systems for protecting buildings against intentional releases of biological agents.

REFERENCES

- ASHRAE. 1993. *1993 ASHRAE Handbook—Fundamentals*. Atlanta: American Society of Heating, Refrigerating and Air-Conditioning Engineers, Inc.
- Gordon, D. 1978. Numerical calculations on viscous flows fields through cylindrical arrays. *Computers & Fluids* 6(1): 1-13.
- IES. 1981. *Lighting Handbook Application Volume*. New York: Illumination Engineering Society.
- Kowalski, W.J., and W.P. Bahnfleth. 2000. Effective UVGI system design through improved modeling. *ASHRAE Transactions* 106(2): 4-15.
- Kowalski, W. J., W.P. Bahnfleth, D. Witham, B.F. Severin, and T.S. Whittam. 2000. Mathematical modeling of UVGI for air disinfection. *Quantitative Microbiology* 2(3): 249-270.
- Kowalski, W.J. 2001. Design and optimization of UVGI air disinfection systems. Ph.D. thesis, The Pennsylvania State University.
- Kundu, P.K. 1990. *Fluid Mechanics*. New York: Academic Press, Inc.
- Lash, D.J. 2000. Performance benefits of highly reflective diffuse materials in lighting fixtures. *J. of Illum. Eng. Soc.* Winter:11-16.

- Lidwell, O.M., and E.J. Lowbury. 1950. The survival of bacteria in dust. *Annual Review of Microbiology* 14: 38-43.
- Linden, K.G., and J.L. Darby. 1994. Ultraviolet disinfection of wastewater: Effect of dose on subsequent reactivation. *Water Res.* 28: 805-817.
- Minitab. 2000. *Minitab Statistical Software Release 13.20*. Minitab, Inc.
- Montgomery, D.C., 2001. *Design and Analysis of Experiments*. New York: John Wiley & Sons, Inc.
- Munakata, N., and C.S. Rupert. 1974. Dark repair of DNA containing spore photoproduct. In *Bacillus subtilis*, *Molec. Gen. Genet.* 130: 239-250.
- Peccia, J., and M. Hernandez. 2001. Photoreactivation in airborne *Mycobacterium parafortuitum*. *Appl. and Environ. Microbiol.* 67.
- Peccia, J., H.M. Werth, S. Miller, and M. Hernandez. 2001. Effects of relative humidity on the ultraviolet induced inactivation of airborne bacteria. *Aerosol Sci. & Technol.* 35: 728-740.
- Rahn, R.O., and J.L. Hosszu. 1969. Influence of relative humidity on the photochemistry of DNA films. *Biochim. Biophys. Acta.* 190: 126-131.
- Rahn, R.O., P. Xu, and S.L. Miller. 1999. Dosimetry of room-air germicidal (254 nm) radiation using spherical actinometry. *Photochem and Photobiol* 70(3), 314-318.
- Rentschler, H.C., R. Nagy, and G. Mouromseff. 1941. Bactericidal effect of ultraviolet radiation. *J. Bacteriol.* 42: 745-774.
- Rentschler, H.C., and R. Nagy. 1942. Bactericidal action of ultraviolet radiation on air-borne microorganisms. *J. Bacteriol.* 44: 85-94.
- Riley, R.L., and J.E. Kaufman. 1972. Effect of relative humidity on the inactivation of airborne *Serratia marcescens* by ultraviolet radiation. *Applied Microbiology* 23(6): 1113-1120.
- Setlow, J.K. 1966. Photoreactivation. *Radiat. Res. Suppl.* 6: 141-155.
- UVDI. 2002. Summary report on bioassay test results for 3 bacterial species under UV exposure performed by Research Triangle Institute. Ultraviolet Devices, Inc.
- Westinghouse. 1982. Booklet A-8968. Westinghouse Electric Corp., Lamp Div.

